ARCHIVES OF MECHANICS
Arch. Mech. **73** (2), 201–215, 2021, DOI: 10.24423/aom.3746

Application of the diagnostic plot in estimation of the skin friction in turbulent boundary layer under an adverse pressure gradient

P. NIEGODAJEW*), A. DRÓŻDŻ, W. ELSNER

*Czestochowa University of Technology, Department of Thermal Machinery, Armii Krajowej 21, 42-200 Czestochowa, Poland, *) e-mail: niegodajew@imc.pcz.pl*

The paper concerns the problem of determining friction velocity in wall-bounded flows affected by an adverse pressure gradient (APG). In the work of Niegodajew *et al.* [22] the corrected Clauser chart method (CCCM) for such flow conditions was proposed. This approach utilises the mean velocity profiles and turbulence intensity profiles to accurately estimate the friction velocity. In another work, Dróżdż *et al.* [27] presented a modified version of the diagnostic-plot scaling (DPS) which allows for direct reconstruction of turbulence intensity profiles based on the local mean velocity profile, even when the flow is affected by a strong pressure gradient. This paper is aimed at verifying whether, when combining both of these methods (i.e. DPS and CCCM), the friction velocity can be accurately determined for APG flow conditions and one can possibly take advantage from both methods. The analysis revealed that the new approach is able to predict the friction velocity with uncertainty less than 5% for all the considered cases for the Clauser–Rotta parameter $\beta < 17$. Lastly, DPS-CCCM was also confronted with two empirical approaches (from available literature) allowing for estimation of the friction velocity under APG conditions. The performance of DPS-CCCM was found to be better than the ones of two other empirical approaches.

Key words: turbulent boundary layer, friction velocity, Clauser-chart, adverse pressure gradient, diagnostic plot.

1. Introduction

A precise measurement of the wall shear stress $\tau_w = \mu(\partial U/\partial y)$ at $y = 0$ is highly important from an engineering point of view as τ_w accounts for a substantial portion of the total drag in ground and air vehicles. Here, μ is the fluid dynamic viscosity, U the streamwise velocity and y the wall-normal distance. At present, there are plenty of experimental techniques that can be used to directly measure the skin friction. The most commonly used is oil-film interferometry (OFI) of Tanner and Blows [1]. Shear stress can be also determined based on a single velocity measurement made using either hot-wire anemometry (HWA) [2] or laser-Doppler anemometry (LDA) techniques [3], which should be

performed at a certain distance normal to the wall within the linear region of the viscous sublayer. PRESTON [4] proposed an approach which relays on a single point measurement of pressure with the Pitot tube very close to the wall. As it was further shown by PATEL [5] the accuracy of this approach (also known as the Preston tube) does not depart much from those of already mentioned methods. A rapid progress in micro-electro-mechanical systems (MEMS) has resulted in the development of micron-sized wall sensors that can be used to measure local skin friction even at high Reynolds numbers [6, 7]. Application of hot-film gauges [8] and MEMS based hot-films [9] have also been proved to be very effective in measurements of the skin friction in steady laminar and turbulent flows. Measurement of wall shear stress can be also performed in liquid flows based on a heating element (electrode) flush-mounted to the wall [10, 11].

Even though the accuracy of all the mentioned methods is rather high [2, 12, 13], they are usually quite difficult to apply in practice. It is because the measurement is performed in the closest vicinity of the wall where very small values of velocity are reported and hence these methods require additional calibration and corrections. Even more problematic is estimation of the wall-shear stress when the flow becomes affected by strong wall-normal fluctuations. Such an effect becomes more pronounced towards higher both, pressure gradient and the Reynolds number, and it is regarded as a serious challenge for all currently available measuring techniques [14].

In 1956, CLAUSER [15] presented an interesting approach (the well-known Clauser-chart method (CCM)) which utilises the mean velocity profile $U^+(y^+)$ to determine the friction velocity $u_\tau = (\tau_w/\rho)^{0.5}$ at the wall by fitting the measured data to the logarithmic region of the turbulent boundary layer (TBL) – assuming the universality of the near-wall region. Here, the superscript $(^+)$ indicates the viscous scales (u_τ) and (ν/u_τ) for U^+ and y^+, respectively, and ρ is the fluid density. This approach, however, is not free of drawbacks: it overestimates the friction velocity for low Reynolds number flows [16] and underestimates it when a flow is affected by a favourable or adverse pressure gradient (APG) [17]. The latter weakness of the CCM is particularly troublesome as most practical flow cases are affected, in particular, by APG, e.g., airfoils, diffusers and turbine blades. There were also attempts aimed at modifying CCM to make it applicable to APG flows [18, 19]. This was met with partial success as the proposed modification did not take into account the flow history effect being responsible for different locations of the outer maximum in the turbulence intensity profiles [20, 21].

A new approach to the problem has been presented by NIEGODAJEW *et al.* [22] who utilised the findings of DECK *et al.* [23] and MARUSIC [24]. In the former work, it was suggested that there is a significant contribution of a large-scales motion (LSM) to the mean wall shear stress, particularly under moderate and

high Reynolds numbers. In the latter work, it was found that the maximum energy of LSMs (for canonical flows) coincides well with the geometrical centres of the logarithmic region. In turn, in [22] the authors found that in APG the mean velocity profiles intersect with the logarithmic line:

$$U^+ = 1/\kappa \ln(y^+) + B \quad \text{(where } \kappa = 0.379 \text{ and } B = 3.56\text{)} \tag{1.1}$$

at the same location as the one where the outer peak in a turbulence intensity profile occurs. Moreover, the amplitude modulation coefficient $\overline{3u_L^+ u_S^{+2}}/u'^3$ (where the subscripts L and S denote the large and small-scale components of the streamwise velocity fluctuations $u(t)$) reaches zero exactly at the same y^+ position. This implies that there is an indirect relationship between LSM and skin friction in APG. This relationship was further used to develop a new approach, the corrected Clauser-chart method (CCCM). According to Niegodajew *et al.* [22], this approach relies on finding a value of u_τ, for which $U^+(y^+)$ profile intersects with the logarithmic line (1.1) at the same y^+ position as the outer maximum in u'. Values of 'von Karman' κ and B constants in relation (1.1) were obtained by fitting U^+ values at the location of the outer maximum $y^+(u'_{max})$ using the experimental data of Monty *et al.* [25] and Dróżdż and Elsner [21], which were obtained under moderate and strong APG, respectively. Taking into account that the CCCM relies upon identifying the wall-normal position of u' maximum, one may conclude that it is insensitive to the flow history changes as this location depends on the flow history and/or local pressure gradient effects [21]. This may be also supported by the studies performed in the previous work [22] in which the authors showed that CCCM allowed estimating proper values of the friction velocities regardless of the flow history. It was proved that the uncertainty of the method is not higher than 2.5% for the Clauser–Rotta parameter $\beta = (\delta^*/\tau_w)(dP_\infty/dx)$ up to 28 and for the friction-based Reynolds number $\mathrm{Re}_\tau = u_\tau \delta/\nu$ above 1800 in the region prior to the APG section. In these relations, δ^* is the displacement thickness, δ the boundary layer thickness at the wall-normal location, dP_∞/dx the streamwise pressure gradient in the free-stream and ν the kinematic viscosity. In our other paper [26], CCCM was also found to accurately predict the friction velocity on a flat surface in APG flow, however, downstream a surface undulation with relatively high amplitude. One should emphasise that as the premultiplied streamwise energy spectra and the amplitude modulation coefficient are difficult to obtain in practice, so the method can rely solely on the u' profile which can be acquired directly from anemometry measurements.

In another work, Dróżdż *et al.* [27] presented an adapted version of the diagnostic-plot scaling (DPS), originally proposed by Alfredsson *et al.* [28], which can be used to reconstruct the turbulence intensity profiles. The authors introduced the shape factor to modify the original formula of Alfreds-

SON *et al.* [28] to make it suitable for strong APG flows up to $\beta < 14$. Hence, it is interesting to verify whether the hybrid approach (CCCM and DPS) can be used to accurately estimate friction velocities in APG flows. If so, information only about the mean velocity profile (measured, for instance, with a pressure probe or when the measurements are affected by spatial and/or temporal averaging [29] which may lead to erroneous estimation of the outer maximum location in turbulence intensity profile) would be sufficient to reconstruct u' with DPS and then to estimate u_τ using CCCM. That is why the purpose of the present paper is to examine performance of such a hybrid (DPS-CCCM) approach based on the available skin friction experimental data obtained under low/medium and strong APG flow conditions. Obtained accuracy of DPS-CCCM has been also confronted with the ones of two empirical approaches allowing for estimation of the friction velocity under APG conditions, namely, the one of FELSCH *et al.* [30] and the other one of WHITFIELD *et al.* [31].

2. Experimental databases and methods

To determine whether the combination of CCCM and DPS is sufficient for accurately estimating u_τ, we examined three different databases which are summarised in Table 1. Note that the experiments of MONTY *et al.* [25] (for the moderate APG flow) and DRÓŻDŻ and ELSNER [21] (for the strong APG flow) were previously investigated in the work on the development of CCCM [22]. Note that there are also other experiments and simulations in APG that have been investigated in our previous work [22], namely the ones from [20, 32–36]. These flow cases are characterised either by too-high shape factor values ($H > 2$), where $H = \delta^*/\theta$, and/or by too-low Reynolds numbers ($\mathrm{Re}_\tau < 1000$) and so are out of the application limit of CCCM and cannot be included in the present study.

In the meantime, however, new databases including the results of skin frictions in APG flows were delivered by VOLINO [37] and by SANMIGUEL VILA *et al.* [38]. In the former work, the upper limit of the results was at $\mathrm{Re}_\tau \approx 1130$. Hence, the CCCM cannot be used to estimate the friction velocity since the method's lower application limit is at $\mathrm{Re}_\tau \approx 1800$ in the area preceding the APG zone, as shown in [22]. In the latter work, some results were obtained at sufficiently high Reynolds numbers under weak APG (see Table 1) so they were included in the present study.

One should note that there is one more specific difference between the experiments of MONTY *et al.* [25] and DRÓŻDŻ and ELSNER [21] and the one of SANMIGUEL VILA *et al.* [38]. Namely, in [21, 25] the boundary layers developed in a way that ensured an almost constant value of Re_τ within the entire APG section. It is, however, not the case in the experiment [38] where within

the low-β range (from 1.24 to 2.43) the boundary layer thickness increased from 52 to 101 mm while u_τ decreased from 0.88 to 0.65 m/s. Consequently, Re_τ increased substantially from 2940 to 4410 for the mentioned β range. However, in a zero-pressure gradient region (prior to the APG zone) the value of Re_τ was ∼1400. Therefore, this experiment should be treated with caution because, for such a low Re_τ, the logarithmic region may not be well developed [39], and the uncertainty in the estimation of u_τ was relatively high – up to 3%. Nonetheless, since the value of Re_τ in APG is much higher for selected cases from the experiment [38] (see Table 1) this data was included in the present study.

It is also important to note that for the given experiments of MONTY *et al.* [25] and DRÓŻDŻ and ELSNER [21], β increases with streamwise distance, so these flow cases should be regarded as non-equilibrium boundary layers. However, the experiment of SANMIGUEL VILA *et al.* [38] is a near-equilibrium boundary layer flow at $\beta \approx 2.4$. More details about near-equilibrium and non-equilibrium boundary layers can be found in [20] and [37], respectively.

As can be seen from Table 1, the data used cover a wide range of flow parameters, i.e.: Re_τ ranges from 1780 to 4410, the momentum thickness-based Reynolds number $\mathrm{Re}_\theta = U_e\theta/\nu$ from 7620 to 23450, β from 0.91 to 17.2, and H from 1.3 to 1.71. In the mentioned relations, U_e is the velocity at the edge of the boundary layer thickness, θ the momentum loss thickness and H the shape factor.

Table 1. Databases used in the present study.

source	symbol	Re_τ	Re_θ	β	H	comments
SANMIGUEL VILA *et al.* [38]	•	2940–4410	12530–23450	1.24–2.43	1.43–1.52	weak APG
MONTY *et al.* [25]	▲	1780–3890	7620–17070	0.91–4.75	1.4–1.61	moderate APG
DRÓŻDŻ and ELSNER [21]	■	1910–3400	9230–22340	2.0–17.2	1.3–1.71	strong APG

As it was shown in the work of NIEGODAJEW *et al.* [22], to calculate u_τ the CCCM requires an accurate estimation of the outer maximum location in the u' profile. So, in this paper we would like to demonstrate that DPS can predict positions of these extrema with satisfying precision. A general DPS formula proposed in [27] takes the following form:

$$\frac{u\prime}{U}\left(\frac{H_0}{H}\right)^n = 0.280 - 0.245\frac{U}{U_e}, \tag{2.1}$$

where H_0 is a constant and equals 1.26, and the value of n-exponent, according to [27], can be calculated using the relation:

$$n = 0.66\ln\left(\frac{\mathrm{d}C_p}{\mathrm{d}x}\delta_{in}\right) + 3.51. \tag{2.2}$$

In the above formula, $C_P = 2(P_e - P_{e,in})/(\rho U_{e,in}^2) = 1 - (U_e/U_{e,in})^2$, the subscript *in* denotes the inlet conditions corresponding to the location where the lowest shape factor occurs, e.g. under zero pressure gradient (ZPG) conditions, which always takes a non-zero value in APG. It is important to note that the log-layer develops in ZPG and this development is accompanied by a decreasing shape factor. The shape factor decreases downstream in ZPG and can start to increase after the flow reaches APG. The local minimum in H (in the configuration from ZPG to APG) can be regarded as the downstream limit for the development of the log-layer, so it was chosen as a representative criterion – at the streamwise location with the lowest H, the log-region is developed the most. Relation (2.1) can be used to reconstruct the outer part of any turbulent intensity profile when the flow is affected by the pressure gradient. The transformed version of Eq. (2.1) that can be used for such a purpose takes the form:

$$u'^{+} = \left(0.280 - 0.245\frac{U^+}{U_e^+}\right)U^+\left(\frac{H}{H_0}\right)^n. \tag{2.3}$$

Note that accurate estimation of n and H in the relation (2.3) is not so important here. The last term in relation (2.3), namely $(H/H_0)^n$ is not responsible for the location of the outer maximum (which is important in CCCM); however it determines predicted values of u'. Formula (2.3) was further used to reconstruct the outer parts of turbulent intensity profiles from experiments characterised by flow parameters in Table 1 in order to obtain friction velocities using CCCM. The value of u_τ, can be obtained by matching the intersection of the $U^+(y^+)$ profile with the logarithmic line (1.1) at the same y^+ position as the y^+ position of the outer maximum in the reconstructed with DPS $u'(y^+)$.

3. Results

The sample results in the form of measured and reconstructed outer regions (only) of turbulence intensity profiles for cases characterised by moderate [25] and strong [21] APG are presented in Fig. 1a and 1b, respectively (symbols are the same as in Table 1). The fit polynomial lines were introduced to better estimate the location of each maximum (as suggested in [22]). As can be seen, formula (2.3) slightly underestimates the wall-normal location of the maximum for the selected data of MONTY *et al.* [25] and it overestimates the wall-normal location for the selected data of DRÓŻDŻ and ELSNER [21] (see the difference between the measured and predicted maxima marked as y^+_{max} in Figs. 1a and 1b). However, as it is further shown, the discrepancies in estimation of local outer maxima (between experiment and the one obtained from formula (2.3)) do not contribute much to uncertainty in obtaining friction velocities.

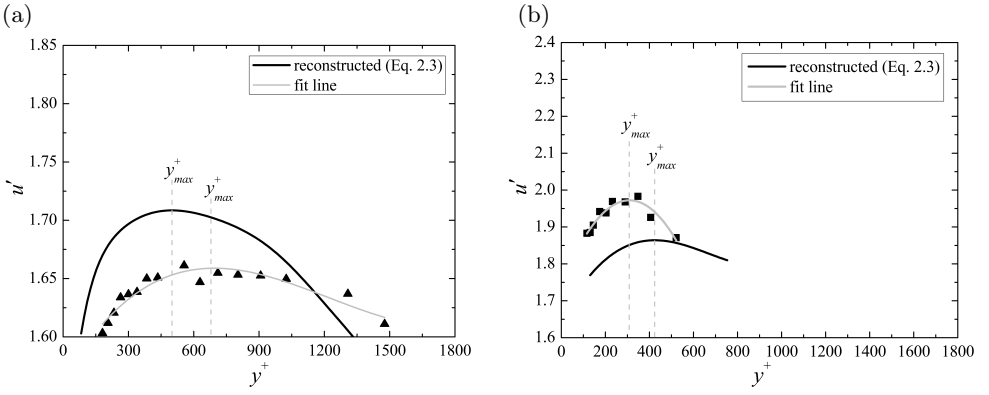

FIG. 1. Actual and predicted y^+ locations of the outer maxima in u' for selected data of: (a) MONTY *et al.* [25] for $\beta = 4.4$ and for $\mathrm{Re}_\theta = 18700$ and (b) DRÓŻDŻ and ELSNER [21] for $\beta = 12.4$ and for $\mathrm{Re}_\theta = 17000$. Symbols as in Table 1.

The locations of maxima determined using DPS can be directly used to estimate the friction velocities using CCCM. For this, one needs to find such a value of u_τ, for which the $U^+(y^+)$ profile intersects with the logarithmic line (1.1) at the same y^+ position as the y^+ position of the outer maximum in the reconstructed with DPS $u'(y^+)$ profile. The friction velocities obtained in this way are collected in Table 2 (see the column named as u_τ DPS Eq. (1.1)) next to the measured ones, along with corresponding uncertainties ε for DPS relative to OFI measurements. Note that, as shown in [27], DPS allows for the reconstruction of turbulence intensity profiles up to $\beta = 14$; however, since there are available OFI measurements for higher β values it is interesting to also examine the performance of the method for such data, i.e. flow cases 20 and 24 in Table 2. As it can be seen, the DPS approach (with logarithmic line (1.1)) allows for the estimation of the friction velocity with uncertainty ε up to 5% for $\beta < 14$. For additional cases 20 and 24 with higher β values, i.e. 17.2 and 16.7, respectively, the uncertainty of DPS for estimating u_τ clearly increased, reaching 6.17% for case 20.

As showed in Fig. 1, the locations of predicted outer maxima differ from those of the experiments. Therefore, it is worth examining whether there is a better fitting logarithmic line than the one described by Eq. (1.1). To verify this, values of U^+ at $y^+(u'_{max})$, with maxima (u'_{max}) determined using DPS as a function of $y^+(u'_{max})$ are plotted in Fig. 2. The new data can be described with a new logarithmic line:

$$U^+ = 1/\kappa \ln(y^+) + B \quad (\text{where } \kappa = 0.388 \text{ and } B = 4.16). \tag{3.1}$$

It is interesting to note that parameters κ and B characterising the new line (3.1) are very close to those commonly used to describe the logarithmic

Table 2. Measured and estimated skin friction velocities using CCM and CCCM methods.

case	Re_τ	β	H	u_τ [m/s] OFI	u_τ [m/s] DPS Eq. (1.1)	u_τ [m/s] DPS Eq. (3.1)	ε [%] DPS Eq. (1.1)	ε [%] DPS Eq. (3.1)	source
1	2937	1.24	1.43	0.854	0.897	0.884	4.97	3.50	weak APG [38]
2	3451	1.80	1.46	0.768	0.799	0.789	3.99	2.69	
3	3831	2.30	1.50	0.683	0.706	0.699	3.31	2.27	
4	4160	2.43	1.52	0.654	0.667	0.661	2.05	1.13	
5	4414	2.19	1.51	0.644	0.658	0.654	2.03	1.49	
6	1860	0.91	1.4	0.461	0.471	0.462	2.02	0.15	moderate APG [25]
7	1940	1.67	1.46	0.375	0.381	0.376	1.65	0.11	
8	1980	3.12	1.53	0.331	0.323	0.319	2.27	3.39	
9	1980	4.74	1.61	0.296	0.295	0.292	0.24	1.25	
10	2500	4.4	1.58	0.389	0.383	0.380	1.47	2.37	
11	3520	4.53	1.54	0.508	0.498	0.493	2.03	2.91	
12	3890	4.4	1.53	0.565	0.548	0.544	2.92	3.75	
13	3090	1.7	1.44	0.625	0.622	0.613	0.46	1.90	
14	2500	1.52	1.45	0.498	0.482	0.476	3.25	4.46	
15	3267	3.22	1.51	0.513	0.493	0.487	3.90	4.98	
16	3560	4.75	1.55	0.535	0.516	0.511	3.50	4.43	
17	2140	2.1	1.36	0.358*	0.366	0.360	2.23	0.56	strong APG [21]
18	2160	5.6	1.43	0.310*	0.317	0.313	2.25	0.96	
19	1910	11.5	1.57	0.252	0.262	0.259	4.17	2.98	
20	1890	17.2	1.71	0.227	0.241	0.239	6.17	5.29	
21	3505	2.0	1.3	0.693*	0.712	0.699	2.69	0.88	
22	3590	5.56	1.39	0.598*	0.606	0.598	1.33	0.01	
23	3400	12.4	1.52	0.475	0.499	0.492	5.07	3.59	
24	3340	16.7	1.61	0.430	0.451	0.447	4.88	3.95	

*Values estimated with an alternative method to OFI, however with an error less than 3% [19].

region of TBL, i.e. $\kappa = 0.38$ and $B = 4.1$ [40]. As it can be seen, the new log-line (3.1) is slightly shifted upward with respect to the original one (1.1). The new line was further used to determine friction velocities to check whether the uncertainty of the hybrid DPS-CCCM can be reduced. The results of the friction velocities obtained using the new line are collected in Table 2 (see the column named u_τ DPS Eq. (3.1)) together with corresponding uncertainties (see the column named ε DPS Eq. (3.1)). One can see that the maximum uncertainty in estimating u_τ when using the log-line (3.1) is at the same level as when using the log-line (1.1), i.e. 5% even when taking into account cases 20 and 24, i.e. for $\beta \approx 17$. To demonstrate the advantage of using line (3.1), the error histogram

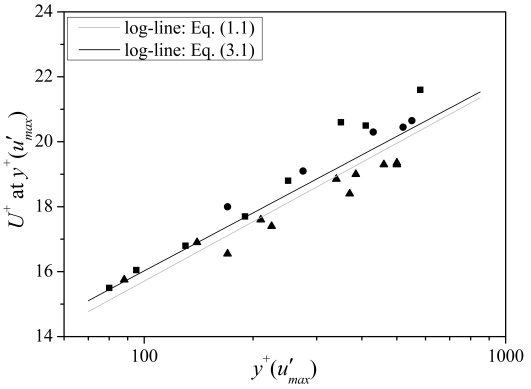

FIG. 2. Values of U^+ at $y^+(u'_{max})$ in the outer region against $y^+(u'_{max})$ – maxima (u'_{max}) obtained using DPS. Symbols as in Table 1.

for the cases from Table 1 (excluding cases 20 and 24 for high β values) is presented in Fig. 3a. As it can be seen, there are more cases with $\varepsilon < 1$ when using DPS-CCCM together with line (3.1) and more cases with $2 < \varepsilon < 3$ when adopting line (1.1). It is because the new log-line (3.1) ensures better approximation of the maxima determined with the use DPS (see Fig. 2). Hence, it is recommended to use log-line (3.1) instead of the original one (1.1) to estimate friction velocity with DPS-CCCM.

The available literature also offers other empirical skin friction laws for arbitrary pressure gradient TBLs. The most popular ones employ two global parameters, i.e. Re_θ and H, like relations of FELSCH *et al.* [30] and the more recent one of WHITFIELD *et al.* [31]. In the former one, the authors formulated the following relation that can be used to calculate the skin friction coefficient:

$$C_f = 0.058\,\mathrm{Re}_\theta^{-0.265}(0.93 - 1.95\log_{10} H)^{1.705}. \tag{3.2}$$

In the latter work, the authors proposed another empirical form for the friction coefficient, namely:

$$C_f = \frac{0.3e^{(-1.33H)}}{(\log_{10}\mathrm{Re}_\theta)^{(1.74+0.31H)}} + 1.1\times 10^{-4}\left(\tanh\left(4 - \frac{H}{0.875}\right) - 1\right). \tag{3.3}$$

The friction coefficient can be directly used to calculate the friction velocity with information about the free stream velocity U_e using the relation:

$$C_f = \frac{2u_\tau^2}{U_e^2}. \tag{3.4}$$

Empirical relations (3.2) and (3.3) were used to calculate friction velocity and the results are presented in Fig. 3a. As can be seen, the performance of each approach

is comparable; however, DPS-CCCM provides a slightly better prediction of u_τ as there are no cases with $\varepsilon > 5$. Our approach differs from the ones of FELSCH *et al.* [30] and WHITFIELD *et al.* [31] as it utilises information about the location of the outer peak instead of the Reynolds number, so it may be a good alternative to these correlations.

As a complement to the data in the histogram, the measured values of u_τ vs the ones estimated using DPS-CCCM with the log-line (3.1), are presented in the form of a parity plot in Fig. 3b. One can see that the uncertainty of the method does not depend on whether the value of friction velocity is high or low since the uncertainty of the results in Fig. 3b is more or less uniform within the range of investigated u_τ values. Note that according to [22], the maximum uncertainty of CCCM is 2.5%, while for the proposed method utilising DPS-CCCM, it is 5%, which still can be regarded as acceptable (especially because the method does not require measurements of turbulence intensity profiles).

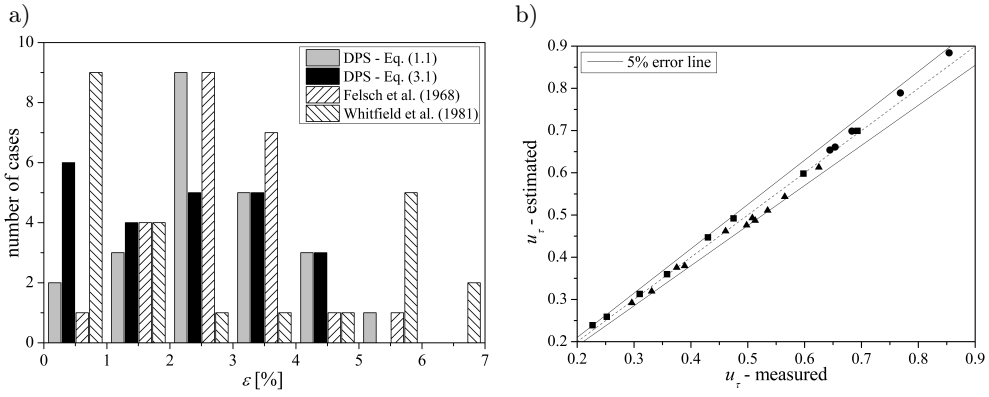

FIG. 3. Histogram of errors for DPS when using line (1.1) and line (3.1) and correlations of: (a) FELSCH *et al.* [30] and WHITFIELD *et al.* [31] and (b) a parity plot showing the relation between the measured and estimated, using DPS with the new log-line (3.1), values of friction velocity (b). Symbols as in Table 1.

Finally, let us turn attention to the cases characterised by low-β values e.g. (1, 2, 6, 7, 14, 17 and 18 – see Table 2) for which the outer maximum was not apparent. This implies an important advantage of DPS-CCCM over CCCM, since it can also be used to estimate u_τ for low values of β. The uncertainty in the mentioned flow cases is not higher than 3.5% (when using log-line (3.1)) – see Table 2.

4. Conclusions

This work demonstrated how the friction velocity can be estimated for flow affected by low/medium and strong APG, where the universal log-law becomes

invalid. The new method is based on two previously introduced procedures i.e. the corrected Clauser-chart method (CCCM) and diagnostic-plot scaling (DPS). The former allows the estimation of u_τ when having both, the mean velocity profile and turbulence intensity profile in the outer zone only. The latter enables the reconstruction of turbulence intensity profiles based solely on the normal distribution of the mean velocity profiles, allowing it to be combined with CCCM. As a result, the friction velocity can be estimated in APG based on, for instance, the mean velocity profile obtained from dynamic pressure measurements using the Prandtl probe – which is a great advantage of this approach.

This paper examined the performance of such a hybrid solution and reveals that the combined DPS-CCCM, with log-line (3.1), allows the friction velocity to be estimated with an uncertainty of less than 5% for all data up to $\beta \approx 17$, which is the upper bound of DPS application. It was found that the combined DPS-CCCM can also be used to estimate u_τ in flow cases characterised by low-β values when the outer maximum in u' is not apparent. The application of the hybrid approach has a lower bound in the friction Reynolds number at the level of about 1400. However, it cannot be accurately estimated based on the present study. It is expected that Re_τ should be high enough to ensure the logarithmic region to be sufficiently wide.

DPS-CCCM provides a slightly better prediction of u_τ than other previously obtained empirical skin friction laws of Felsch *et al.* [30] and Whitfield *et al.* [31]. More importantly, however, is that the new approach in contrast to simple correlations relays on different concept. Namely, it is based on the recently observed physical phenomenon indicating that the mean wall-shear stress are highly dependent on large-scales motion (LSM) particularly under moderate and high Reynolds numbers.

Another advantage of CCCM-DPS over above mentioned approaches is that it may rely solely on the mean streamwise velocity profile measured in the outer region only. Whereas, empirical correlations of Felsch *et al.* [30] and Whitfield *et al.* [31] require measurement of entire profile for accurate estimation of the shape factor and the Reynolds number based on the momentum loss thickness.

One may also distinguish an advantage of CCCM-DPS over original CCCM, namely, when the measurements are affected by spatial and temporal averaging and as a result estimation of the outer maximum location in a turbulence intensity profile may be wrongly determined and therefore the value of u_τ.

The new DPS-CCCM has been proved to be ready to use in prediction of the friction velocity under the APG flow condition when only the information about the mean streamwise velocity profile is available.

Acknowledgements

The investigation was supported by National Science Centre under Grant No. DEC-2017/25/B/ST8/02480 and by Polish Ministry of Science and Higher Education under scientific research funds No. BS-PB-1-100-3011/2021/P. Ministry of Science and Higher Education (Poland) is also gratefully acknowledged for providing the scholarship for young outstanding scientists No. STYP/15/0246/E-358/2020 to dr Paweł Niegodajew.

References

1. L.H. Tanner, L.G. Blows, *A study of the motion of oil films on surfaces in air flow, with application to the measurement of skin friction*, Journal of Physics E: Scientific Instruments, **9**, 194–202, 1976, https://doi.org/10.1088/0022-3735/9/3/015.
2. N. Hutchins, K.S. Choi, *Accurate measurements of local skin friction coefficient using hot-wire anemometry*, Progress in Aerospace Sciences, **38**, 421–446, 2002, https://doi.org/10.1016/S0376-0421(02)00027-1.
3. E.-S. Zanoun, L. Jehring, C. Egbers, *Three measuring techniques for assessing the mean wall skin friction in wall-bounded flows*, Thermophysics and Aeromechanics, **21**, 179–190, 2014, https://doi.org/10.1134/S086986431402005X.
4. J.H. Preston, *The determination of turbulent skin friction by means of pitot tubes*, The Journal of the Royal Aeronautical Society, **58**, 109–121, 1954, https://doi.org/10.1017/s0368393100097704.
5. V.C. Patel, *Calibration of the Preston tube and limitations on its use in pressure gradients*, Journal of Fluid Mechanics, **23,** 185–208, 1965, https://doi.org/10.1017/S0022112065001301.
6. H. Nagib, C. Christophorou, J.-D. Ruedi, P. Monkewitz, J. Osterlund, S. Gravante, K. Chauhan, I. Pelivan, *Can we ever rely on results from wall-bounded turbulent flows without direct measurements of wall shear stress?,* 24th AIAA Aerodynamic Measurement Technology and Ground Testing Conference, 2004, https://doi.org/10.2514/6.2004-2392.
7. J.D. Ruedi, H. Nagib, J. Österlund, P.A. Monkewitz, *Unsteady wall-shear measurements in turbulent boundary layers using MEMS*, Experiments in Fluids, **36**, 2004, 393–398, https://doi.org/10.1007/s00348-003-0666-1.
8. A.N. Menendez, B.R. Ramaprian, *On the measurement of skin friction in unsteady boundary layers using a flush-mounted hot-film gage*, Journal of Fluid Mechanics, **161**, 139–159, 1984.
9. J.D. Ruedi, H. Nagib, J. Österlund, P.A. Monkewitz, *Evaluation of three techniques for wall-shear measurements in three-dimensional flows*, Experiments in Fluids, **35**, 389–396, 2003, https://doi.org/10.1007/s00348-003-0650-9.
10. J.E. Mitchell, T.J. Hanratty, *A study of turbulence at a wall using an electrochemical wall shear-stress meter*, Journal of Fluid Mechanics, **26**, 199–221, 1966, https://doi.org/10.1017/S0022112066001174.

11. J. Havlica, D. Kramolis, F. Huchet, *A revisit of the electro-diffusional theory for the wall shear stress measurement*, International Journal of Heat and Mass Transfer, **165**, 2021, https://doi.org/10.1016/j.ijheatmasstransfer.2020.120610.

12. A. Segalini, J.-D. Rüedi, P.A. Monkewitz, *Systematic errors of skin-friction measurements by oil-film interferometry*, Journal of Fluid Mechanics, **773**, 298–326, 2015, https://doi.org/doi:10.1017/jfm.2015.237.

13. S. Rezaeiravesh, R. Vinuesa, M. Liefvendahl, P. Schlatter, *Assessment of uncertainties in hot-wire anemometry and oil-film interferometry measurements for wall-bounded turbulent flows*, European Journal of Mechanics, B/Fluids, **72**, 57–73, 2018, https://doi.org/10.1016/j.euromechflu.2018.04.012.

14. R. Örlü, R. Vinuesa, *Instantaneous wall-shear-stress measurements: Advances and application to near-wall extreme events*, Measurement Science and Technology, **31**, 2020, https://doi.org/10.1088/1361-6501/aba06f.

15. F.H. Clauser, *The turbulent boundary layer*, Advances in Applied Mechanics, **4**, 1–51, 1956, https://doi.org/10.1016/S0065-2156(08)70370-3.

16. R.F. Blackwelder, J.H. Haritonidis, *Scaling of the bursting frequency in turbulent boundary layers*, Journal of Fluid Mechanics, **132**, 87–103, 1983, https://doi.org/10.1017/S0022112083001494.

17. R. Madad, Z. Harun, K. Chauhan, J.P. Monty, I. Marusic, *Skin friction measurement in zero and adverse pressure gradient boundary layers using oil film interferometry*, 17th Australian Fluid Mechanics Conference, 2010.

18. S.A. Dixit, O.N. Ramesh, *Determination of skin friction in strong pressure-gradient equilibrium and near-equilibrium turbulent boundary layers*, Experiments in Fluids, **47**, 1045–1058, 2009, https://doi.org/10.1007/s00348-009-0698-2.

19. A. Dróżdż, W. Elsner, D. Sikorski, S*kin friction estimation in a strong decelerating flow*, Journal of Theoretical and Applied Mechanics, **56**, 365–376, 2018, https://doi.org/10.15632/jtam-pl.56.2.365.

20. A. Bobke, R. Vinuesa, R. Örlü, P. Schlatter, *History effects and near equilibrium in adverse-pressure-gradient turbulent boundary layers*, Journal of Fluid Mechanics, **820**, 667–692, 2017, https://doi.org/10.1017/jfm.2017.236.

21. A. Dróżdż, W. Elsner, *An experimental study of turbulent boundary layers approaching separation*, International Journal of Heat and Fluid Flow, **68**, 337–347, 2017, https://doi.org/10.1016/j.ijheatfluidflow.2017.10.003.

22. P. Niegodajew, A. Dróżdż, W. Elsner, *A new approach for estimation of the skin friction in turbulent boundary layer under the adverse pressure gradient conditions*, International Journal of Heat and Fluid Flow, **79**, 108456, 2019, https://doi.org/10.1016/j.ijheatfluidflow.2019.108456.

23. S. Deck, N. Renard, R. Laraufie, P.-É. Weiss, *Large-scale contribution to mean wall shear stress in high-Reynolds-number flat-plate boundary layers up to 13650*, Journal of Fluid Mechanics, **743**, 202–248, 2014, https://doi.org/10.1017/jfm.2013.629.

24. I. Marusic, R. Mathis, N. Hutchins, *High Reynolds number effects in wall turbulence*, International Journal of Heat and Fluid Flow, **31**, 418–428, 2010, https://doi.org/10.1016/j.ijheatfluidflow.2010.01.005.

25. J.P. Monty, Z. Harun, I. Marusic, *A parametric study of adverse pressure gradient turbulent boundary layers*, International Journal of Heat and Fluid Flow, **32**, 575–585, 2011, https://doi.org/10.1016/ j.ijheatfluidflow.2011.03.004.

26. A. Dróżdż, P. Niegodajew, M. Romańczyk, V. Sokolenko, W. Elsner, *Effective use of the streamwise waviness in the control of turbulent separation*, Experimental Thermal and Fluid Science, **121**, 110291, 2021, https://doi.org/10.1016/ j.expthermflusci.2020.110291.

27. A. Dróżdż, P. Niegodajew, W. Elsner, R. Vinuesa, R. Örlü, P. Schlatter, *A description of turbulence intensity profiles for boundary layers with adverse pressure gradient*, European Journal of Mechanics B/Fluids, **84C**, 470–477, 2020, https://doi.org/https://doi.org/10.1016/j.euromechflu.2020.07.003.

28. P.H. Alfredsson, R. Örlü, A. Segalini, *A new formulation for the streamwise turbulence intensity distribution in wall-bounded turbulent flows*, European Journal of Mechanics B/Fluids, **36**, 167–175, 2012, https://doi.org/10.1016/j.euromechflu.2012.03.015.

29. N. Hutchins, T.B. Nickels, I. Marusic, M.S. Chong, *Hot-wire spatial resolution issues in wall-bounded turbulence*, Journal of Fluid Mechanics, **635**, 103, 2009, https://doi.org/10.1017/S0022112009007721.

30. K.O. Felsch, D. Geropp, A. Walz, *Method for turbulent boundary layer prediction*, AFOSR-LFP-Stanford Conference, **1**, 170, 1968.

31. D.L. Whitfield, T.W. Swafford, J.L. Jacocks, *Calculation of turbulent boundary layers with separation, reattachment, and viscous-inviscid interaction*, AIAA Paper, **19**, 1315–1322, 1981.

32. Y. Nagano, T. Tsuji, T. Houra, *Structure of turbulent boundary layer subjected to adverse pressure gradient*, International Journal of Heat and Fluid Flow, **19**, 563–572, 1998, https://doi.org/10.1016/S0142-727X(98)10013-9.

33. A. Dróżdż, W. Elsner, S. Drobniak, *Scaling of streamwise Reynolds stress for turbulent boundary layers with pressure gradient*, European Journal of Mechanics B/Fluids, **49**, 137–145, 2015, https://doi.org/http://dx.doi.org/10.1016/j.euromechflu.2014.08.002.

34. S.H. Hosseini, R. Vinuesa, P. Schlatter, A. Hanifi, D.S. Henningson, *Direct numerical simulation of the flow around a wing section at moderate Reynolds number*, International Journal of Heat and Fluid Flow, **61**, 117–128, 2016, https://doi.org/10.1016/ j.ijheatfluidflow.2016.02.001.

35. A.G. Gungor, Y. Maciel, M.P. Simens, J. Soria, *Scaling and statistics of large-defect adverse pressure gradient turbulent boundary layers*, International Journal of Heat and Fluid Flow, **59**, 109–124, 2016, https://doi.org/10.1016/j.ijheatfluidflow.2016.03.004.

36. J.H. Lee, *Large-scale motions in turbulent boundary layers subjected to adverse pressure gradients*, Journal of Fluid Mechanics, **810**, 323–361, 2017, https://doi.org/10.1017/ jfm.2016.715.

37. R.J. Volino, *Non-equilibrium development in turbulent boundary layers with changing pressure gradients*, Journal of Fluid Mechanics, **897**, A2, 2002, https://doi.org/ 10.1017/jfm.2020.319.

38. C. Sanmiguel Vila, R. Vinuesa, S. Discetti, A. Ianiro, P. Schlatter, R. Örlü, *Experimental realisation of near-equilibrium adverse-pressure-gradient turbulent boundary*

layers, Experimental Thermal and Fluid Science, **112**, 109975, 2020, https://doi.org/10.1016/j.expthermflusci.2019.109975.

39. R. Mathis, N. Hutchins, I. Marusic, *Large-scale amplitude modulation of the small-scale structures in turbulent boundary layers*, Journal of Fluid Mechanics, **628**, 311–337, 2009, https://doi.org/10.1017/S0022112009006946.

40. J.M. Österlund, A. V. Johansson, H.M. Nagib, M.H. Hites, *A note on the overlap region in turbulent boundary layers*, Physics of Fluids, **12**, 1–4, 2000, https://doi.org/10.1063/1.870250.

Received January 13, 2021; revised version March 2, 2021.
Published online April 29, 2021.